Paper submitted December 1986

Grain Noise Suppression through Bandpass Filtering

by P. M. Shankar,* U. Bencharit,* N. M. Bilgutay,* and J. Saniie†

Abstract

Ultrasonic nondestructive evaluation (NDE) of materials is limited by the presence of the backscattered echoes from the grain boundaries (i.e., grain noise). This noise often masks the signal from the flaw, leading to difficulties in its detection and identification. It is shown that in NDE applications where the received noise is primarily due to Rayleigh scattering (from the grain boundaries) and the flaw echo can be represented by a delta function, flaw visibility can be improved significantly (without the need for sophisticated signal-processing algorithms) by merely bandpass filtering (BPF) the lower edge of the received echo spectrum. Both theoretical analysis and experimental results are presented to support this conclusion. The limitations of this technique are also discussed.

INTRODUCTION

Ultrasonic evaluation of metals is impaired by the presence of grains that introduce unwanted echoes to the received signal. Grain noise consists of the backscattered ultrasonic energy from the grain boundaries. This noise often masks the target signal, making identification of flaws difficult.[1-4] A number of techniques have been proposed to combat grain noise and increase the flaw echo-to-grain noise ratio. These techniques include spatial compounding, frequency compounding, split-spectrum processing, etc.[1-4]

In these techniques, a number of decorrelated signals from the target region are obtained, either by scanning the region from different spatial locations of the transducer (spatial compounding), by transmitting over different frequencies (frequency compounding), or by transmitting a wideband signal and then splitting the received spectrum into a number of different frequency bands (split-spectrum technique). These signals are then processed using algorithms such as averaging, minimization, maximization, etc.

Experimental results have shown significant improvement in the flaw visibility through grain noise suppression, especially in the case of nonlinear algorithms.[1,3,4] However, for most flaws, like holes, cracks, etc., simple filtering algorithms[5,6] may be sufficient to improve the signal-to-noise ratio (SNR) (or flaw echo-to-grain noise ratio). The conditions under which the filtering approach provides improvement will be examined to establish the usefulness of the technique.

*Dept. of Electrical and Computer Engineering, Drexel University, Philadelphia, PA 19104; (215) 895-2241.
†Dept. of Electrical and Computer Engineering, Illinois Institute of Technology, Chicago, IL 60616.

THEORY

In most nondestructive evaluation (NDE) applications, the flaw can be considered as constituting a sharp boundary surrounded by grains. The flaw can, therefore, be modeled as a delta function as long as it is not oriented at an acute angle to the direction of propagation of the acoustic field. The received echo $r(t)$ from the target region then becomes

$$r(t) = [A\,\delta(t) + n(t)] * h(t) \tag{1}$$

where $0 \leq t \leq T$, $n(t)$ is the grain noise, $h(t)$ is the impulse response of the transducer, A is a weighing factor, and T is the time duration of the received signal. The Fourier transform of Equation 1 gives Equation 2:

$$R(f) = [A + N(f)]\,H(f) \tag{2}$$

where $-\infty < f < \infty$.

The properties of the individual spectral components in Equation 2 may be examined more precisely by including the effects of absorption and scattering, as shown in Figure 1. Rayleigh scattering, which results from grains that have sizes smaller than the wavelength of the incident acoustic radiation causes grain noise. Under these conditions, the grain noise power varies as the fourth power of the frequency, and the energy loss due to absorption in the material increases exponentially with frequency.[7] Therefore, the grain noise magnitude spectrum will be proportional to the product of the two terms

$$N(f) \propto f^2 \cdot \exp(-bf) \tag{3}$$

where b is a constant. Hence, the noise spectrum will have most of its power in the high-frequency region of the transducer pass band, as shown in Figure 1a. Because the flaw signal is also affected by absorption, its magnitude spectrum $B(f)$ cannot be constant A, as defined in Equation 2, but will decay exponentially with frequency:

$$B(f) \propto \exp(-cf) \tag{4}$$

where c is a constant. Thus, the flaw signal will have a stronger low-frequency content, as shown in Figure 1b. Because the transducer transfer function $H(f)$ has a bandpass spectrum as shown in Figure 1, the received signal spectrum $R(f)$ will also be bandpass.

0025-5327/88/$2.00/0

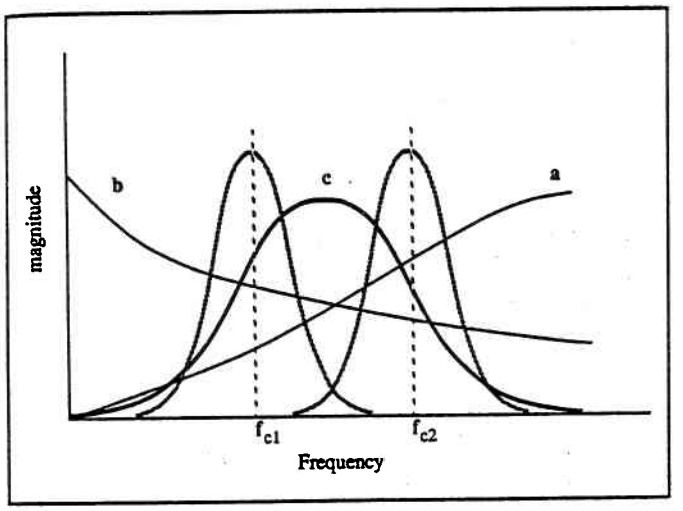

Figure 1—Spectral components of the received signal and bandpass filters with center frequencies f_{c1} and f_{c2}: (a) grain noise spectrum N(f); *(b) flaw spectrum* B(f); *and (c) transducer transfer function* H(f).

Consider now a bandpass filter of width Δf, with its center frequency f_{c1} close to the lower end of the pass band of $R(f)$ (Figure 1). Because the grain noise is mainly of high-frequency content, such a filter can extract the flaw signal. A bandpass filter is preferable to a low-pass filter because it will also remove any low-frequency noise present from other sources. On the other hand, a bandpass filter at the upper end of $R(f)$ centered at f_{c2} will retain mainly grain noise and hence reduce the detectability of the signal. Therefore, when the flaw and grain signals behave as described above, filtering the received signal spectrum with a properly selected bandpass filter will be effective in suppressing the unwanted grain noise.

Although the bandpass filtering (BPF) technique can be very effective, it must be applied diligently. More complicated signal-processing techniques will be necessary if the grain noise is generated from non-Rayleigh scattering processes. Such situations arise in composite materials where the grains form a semiperiodic random orientation or in materials where the grains are Poisson-distributed, in which case the noise spectrum will be broader, making it difficult to choose the desired bandpass frequencies.

In addition, when the average grain size is much larger than the wavelength, BPF will be ineffective because the flaw and the noise spectra will show significant overlap. The geometry and location of the flaw are also important. If the flaw is near the scanning surface, its spectrum will exhibit far less attenuation at high frequencies. Therefore, the flaw and grain spectra will have larger overlap, making the BPF approach less effective. In addition, the bandwidth of the bandpass filter should be chosen so that the resolution is not affected adversely.

PROCEDURE

SNR Enhancement Measurements

Because the purpose of this technique is to enhance the flaw visibility by increasing the magnitude contrast between the flaw and the grain echoes, the SNR can be defined (Equation 5) as the ratio of the peak signal value (i.e., the flaw echo) over the root-mean-square (RMS) grain noise, excluding the flaw region:

$$\text{SNR} = \frac{\text{signal}_{pk}}{\text{RMS.}} \tag{5}$$

Experimentally, this procedure will eliminate leakage of the flaw energy into the grain noise. The SNR of the input and the upper-bandpass filtered signals are similarly measured.

Data-Acquisition System

The experimental data are obtained using the data-acquisition system shown in Figure 2. In the setup, the same transducer is used for transmitting and receiving the ultrasonic wave. The received echoes are digitized and time-averaged in the LeCroy 9400 digital scope to remove the time-varying noise before the data are transferred to the Masscomp MC-500 computer, where further processing is performed.

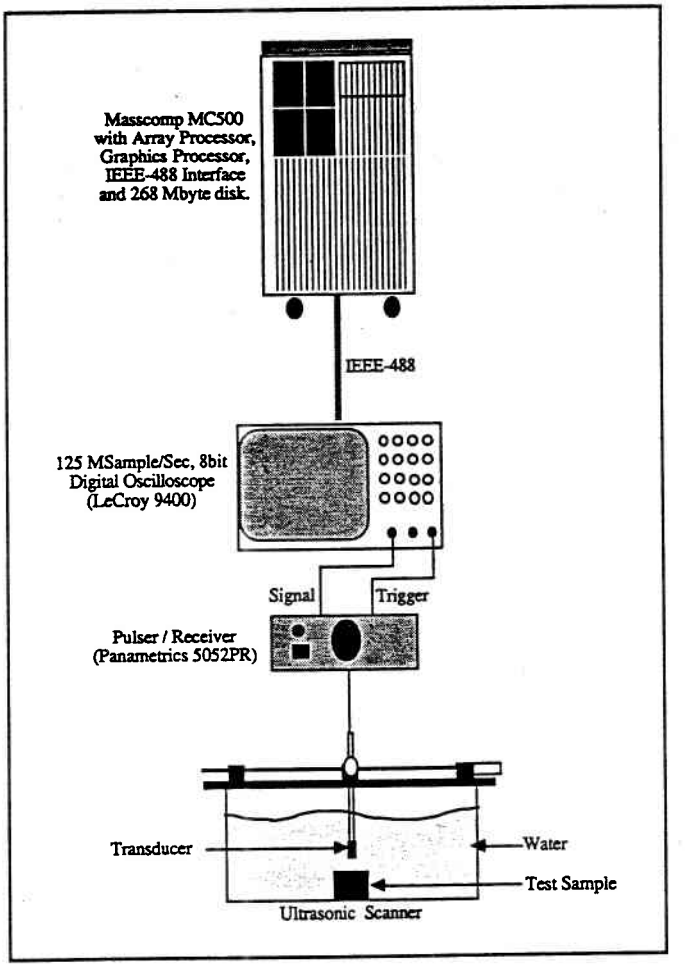

Figure 2—Data-acquisition system.

Experimental Results

The theoretical concepts discussed above were tested using stainless steel and titanium samples with flat-bottom holes representing the flaw. The samples were type 303 heat-treated austenitic stainless steel and titanium with average grain spacing (based on the linear intercept method) of 75 μm, 160 μm, and 15 μm, respectively (the actual grain diameters are approximately a factor of 2 larger than these values).[4] Because the ultrasonic wavelength in these samples is on the order of 1 mm for the transducer used, the incident energy will lead to Rayleigh scattering. Furthermore, because the flat-bottom holes consist of distinct and clearly defined boundaries within the sample, their echoes may be represented by delta functions. Therefore, the experimental data obtained from these samples will be suitable for testing the feasibility of BPF to improve flaw visibility.

Figure 3a shows an A-scan obtained from the stainless steel

sample consisting of 75 μm average grain size and a 3.18 mm flat-bottom hole located at a depth of 60.5 mm from the front surface. The data were obtained by immersion testing using a 0.50 in. (1.27 cm) dia 5 MHz (2 MHz half-power bandwidth) transducer with a sampling frequency of 50 MHz. The corresponding magnitude spectrum is shown in Figure 3b. The flaw signal in Figure 3a is similar in size to the grain echoes and therefore cannot be distinguished without further processing. Figure 3c shows the A-scan corresponding to the lower spectral region of the data in Figure 3a, obtained using a bandpass filter having a 3 dB bandwidth of Δf = 1.75 MHz and a center frequency of f_{c1} = 2 MHz. As a result of significant suppression in grain echoes, the flaw signal can now be identified clearly.

It should be noted, however, that the bandpass-filtered A-scan has smaller bandwidth and, consequently, lower resolution. Conversely, when the upper spectral region of the wideband signal is examined using a bandpass filter with f_{c2} = 4.6 MHz and Δf = 3.5 MHz, the resulting signal (in Figure 3d) corresponds primarily to grain echoes and the flaw amplitude is reduced. (The SNR values before and after the filtering are provided in captions to the corresponding figures).

Similar results were obtained for the stainless steel sample consisting of 160 μm average grain size with a 4.22 mm flat-bottom hole at a 67.3 mm depth. Figures 4a and 4b show the received wideband signal and its magnitude spectrum, respectively. The A-scans corresponding to the lower and upper spectral regions are shown in Figures 4c and 4d. The scans were obtained using bandpass filters with f_{c1} = 3.5 MHz, Δf = 1.75 MHz and f_{c2} = 6.1 MHz, Δf = 2.6 MHz, respectively. Again, the lower spectral region is seen to contain frequencies that favor the flaw signal over the grain echoes whereas the reverse is true for the signal from the upper spectral region.

Experimental data were also obtained for a titanium sample consisting of 15 μm average grain size. Figure 5a shows an A-scan of the titanium sample with a 0.06 in. (1.6 mm) side-drilled hole at 0.75 in. (19.1 mm) depth. The magnitude spectrum of the A-scan is shown in Figure 5b. The spectrum of Figure 5a was divided into lower and upper spectral regions using bandpass filters of f_{c1} = 3.7 MHz, Δf = 1.95 MHz and f_{c2} = 6.2 MHz, Δf = 2.3 MHz, respectively. The corresponding A-scans for the upper and lower spectral regions are shown in Figures 5c and 5d, respectively. It is interesting to note that in this case the two filtered signals show only minor variations. In the titanium sample, the ratio of ultrasonic wavelength to the average grain size is much larger than in the two stainless steel samples (i.e., approximately 5–10 times); consequently, the grain noise resulting from Rayleigh scattering will manifest itself in the higher-frequency range outside the transducer bandwidth, thus making BPF unnecessary (as the transducer itself acts as a filter removing the high-frequency grain noise). To demonstrate this high-frequency nature of the grain noise in the titanium sample and to show the effect of BPF, another set of data is collected from the same titanium sample using a 0.50 in. (12.7 mm) dia high-frequency (10 MHz Gamma) transducer. The A-scan of the sample and its spectrum are shown in Figures 6a and 6b. The filtered signals are shown in Figures 6c and 6d. The lower spectral region was extracted using a bandpass filter with center frequency and bandwidth of f_{c1} = 5.1 MHz and Δf = 3.1 MHz; BPF for the upper region has f_{c2} = 12.1 MHz and Δf = 5.6 MHz, respectively. As shown in these figures, the flaw and the grain echoes occupy different spectral regions and the lower-bandpass filter improves the SNR of the original broadband signal.

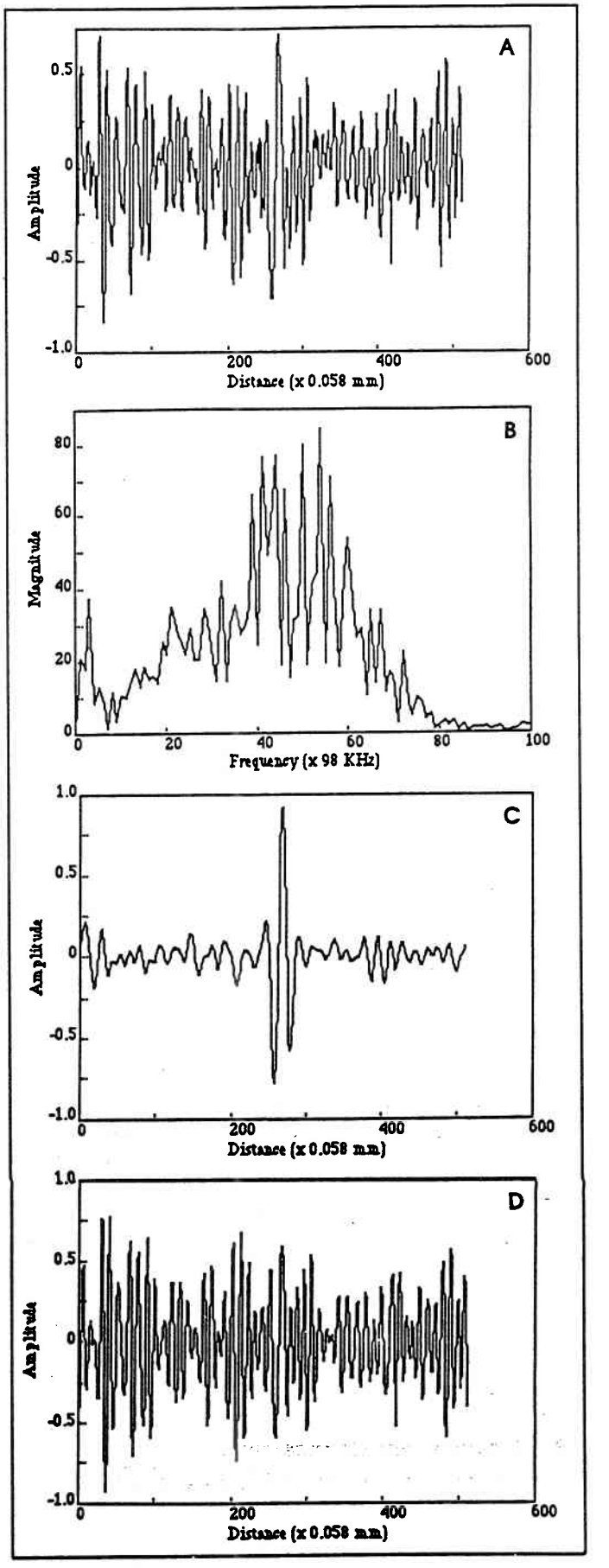

Figure 3—Stainless steel data obtained using 5 MHz transducer (75 μm average grain size): (a) broadband A-scan signal (SNR = 3.58); (b) FFT spectrum of broadband signal; (c) lower-bandpass filtered signal (SNR = 16.94); and (d) upper-bandpass filtered signal (SNR = 0.98).

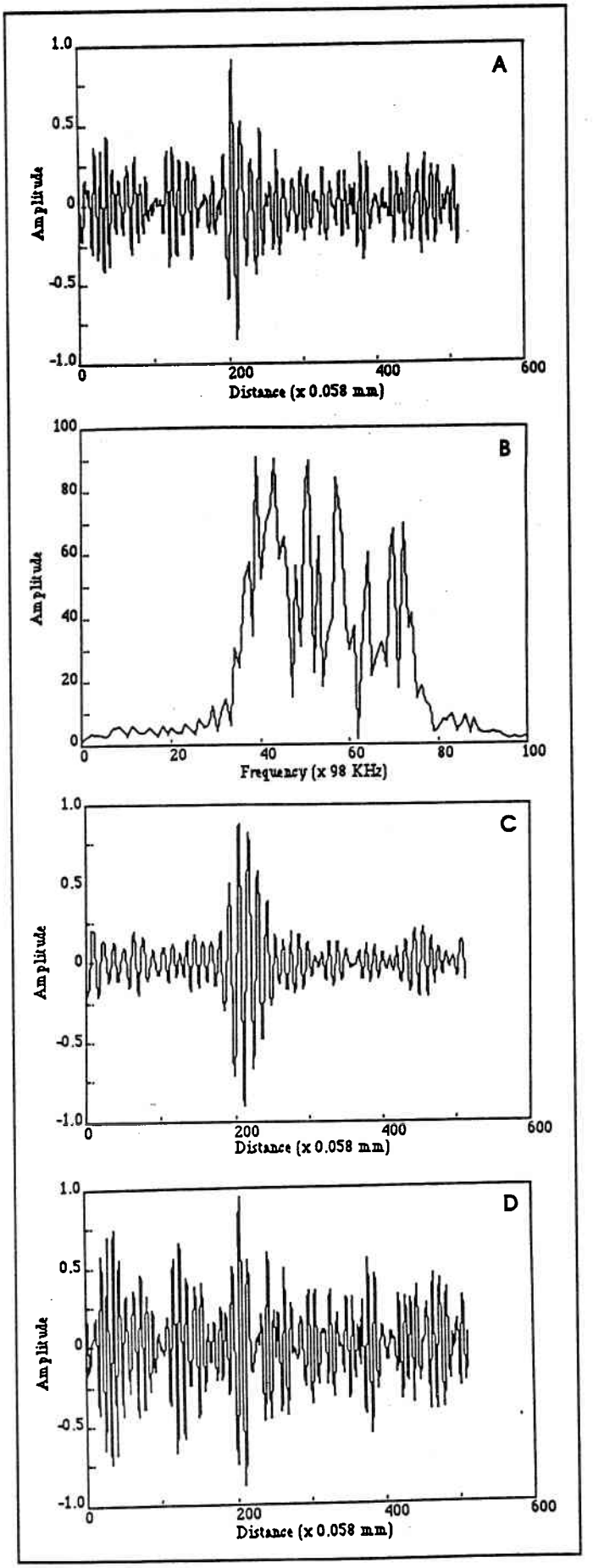

Figure 4—Stainless steel data obtained using 5 MHz transducer (160 μm average grain size): (a) broadband A-scan signal (SNR = 5.03); (b) FFT spectrum of broadband signal; (c) lower-bandpass filtered signal (SNR = 10.86); and (d) upper-bandpass filtered signal (SNR = 2.92).

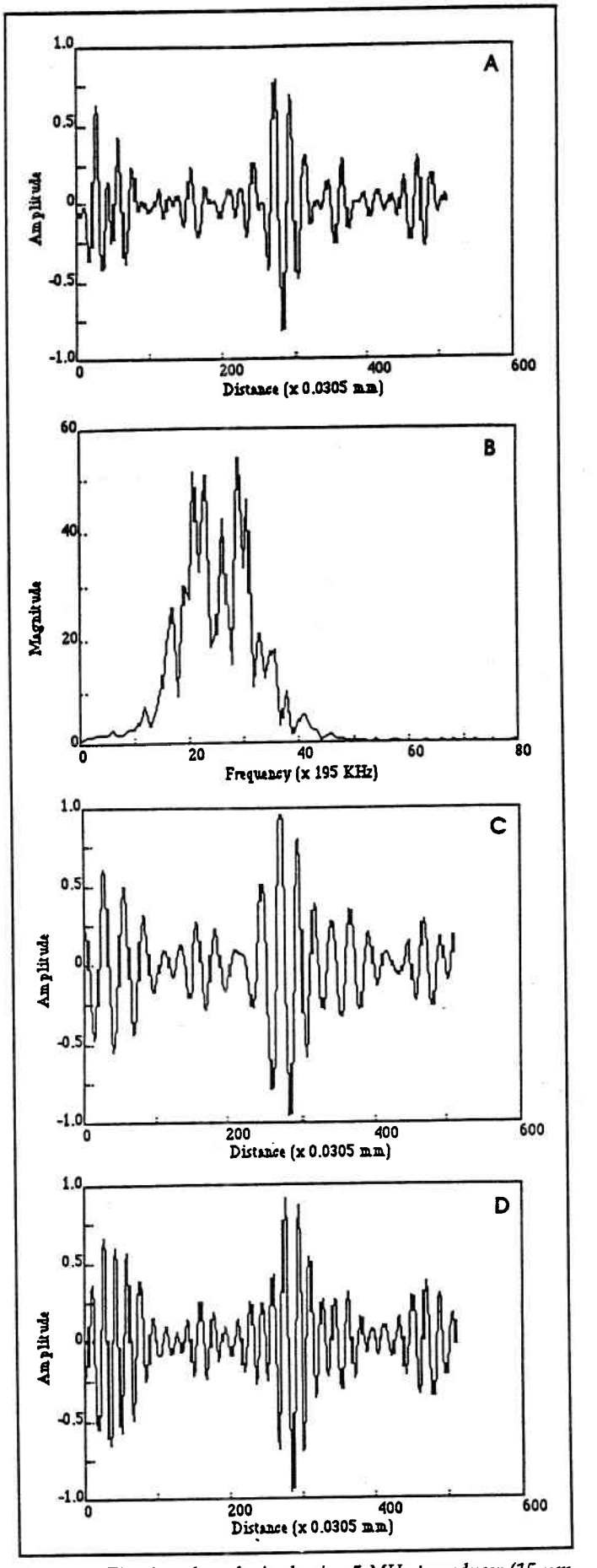

Figure 5—Titanium data obtained using 5 MHz transducer (15 μm average grain size): (a) broadband A-scan signal (SNR = 6.18); (b) FFT spectrum of the broadband signal; (c) lower-bandpass filtered signal (SNR = 5.20); and (d) upper-bandpass filtered signal (SNR = 4.90).

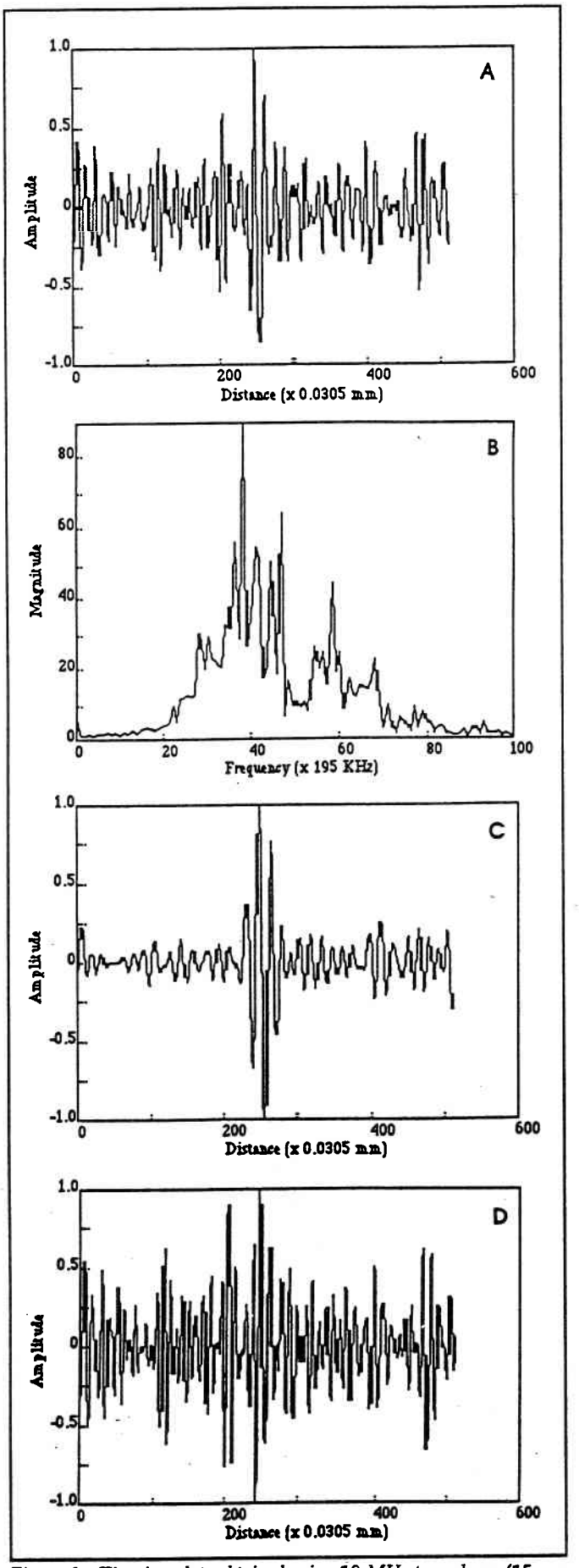

Figure 6—Titanium data obtained using 10 MHz transducer (15 μm average grain size): (a) broadband A-scan signal (SNR = 4.94); (b) FFT spectrum of broadband signal; (c) lower-bandpass filtered signal (SNR = 11.44); and (d) upper-bandpass filtered signal (SNR = 2.68).

CONCLUSIONS

The work presented here shows preliminary results of the BPF technique. Extensive research is under way to determine the range of frequencies of the flaw and grain echoes. The experimental data shown were obtained using typical off-the-shelf transducers. However, if the spectral distribution of the flaw and grain signals is known, then a customized transducer may be more desirable.

The experimental results presented agree with the theoretical analysis and clearly show that BPF is a viable and practical method for grain noise suppression in samples when the flaw and grain spectra occupy distinct frequency regions. When these conditions are valid, BPF can provide improvement similar to that of the more sophisticated algorithms currently being used. In addition, the BPF approach can be achieved readily in real time by hardware implementation, which may be difficult or impossible for other signal-processing algorithms. The results shown can be readily extended to B-scan imaging by using either a series of one-dimensional bandpass filters on each A-scan signal or a two-dimensional bandpass filter[6] on the two-dimensional format data.

Acknowledgment

This work was supported by NSF Grant No. ECS-8505153.

References

1. Newhouse, V. L., N. M. Bilgutay, J. Saniie, and E. S. Furgason, "Flaw-to-Grain Echo Enhancement by Split-Second Processing," *Ultrasonics*, Vol. 20, Mar. 1982, pp 49–68.
2. Magnin, P. A., O. T. Von Ramm, and F. L. Thurstone, "Frequency Compounding for Speckle Contrast Reduction in Phased Array Images," *Ultrasonic Imaging*, Vol. 4, 1982, pp 267–281.
3. Amir, I., N. M. Bilgutay, and V. L. Newhouse, "Analysis and Comparison of Some Frequency Compounding Algorithms for the Reduction of Ultrasonic Clutter," *Transactions of the IEEE*, Vol. UFFC-33, July 1986, pp 402–411.
4. Bilgutay, N. M., and J. Saniie, "The Effect of Grain Size on Flaw Visibility Enhancement Using Split-Spectrum Processing," *Materials Evaluation*, Vol. 42, No. 6, May 1984, pp 808–814.
5. Elsley, R. K., K. W. Fertig, J. M. Richardson, and F. Cohen-Tenoudji, "Statistical Approach to Automatic Flaw Detection," in *Proceedings, 1984 IEEE Ultrasonics Symposium*, Dallas, TX, pp 912–916.
6. Bencharit, U., J. L. Kaufman, N. M. Bilgutay, and J. Saniie, "Frequency and Spatial Compounding Techniques for Improved Ultrasonic Imaging," paper presented at 1986 Ultrasonics Symposium, Williamsburg, VA, Nov. 1986.
7. Krautkramer, J., and H. Krautkramer, *Ultrasonic Testing of Materials*, 1983. Springer-Verlag, Berlin, FRG.

Authors

P. M. Shankar received his M. Tech. in applied optics and his Ph.D. in electrical engineering from the Indian Institute of Technology, Delhi, India, in 1975 and 1980, respectively. He was a postdoctoral fellow at the School of Electrical Engineering, Sydney, Australia, from July 1981 to November 1982. Shankar is presently on the faculty of the Dept. of Electrical and Computer Engineering, Drexel University, Philadelphia, PA. His research interests are optics and ultrasonics.

U. Bencharit received a B.S. in electrical engineering from Lehigh University, Bethlehem, PA, in 1984. He has subsequently been a graduate student at Drexel University, receiving his M.S. in electrical engineering in 1987. Bencharit is currently employed in Thailand.

N. M. Bilgutay received a B.S. degree in electrical engineering from Bradley University, Peoria, IL, in 1973 and M.S. and Ph.D. degrees in electrical engineering from Purdue University, Lafayette, IN, in 1975 and 1981, respectively. Currently, he is an associate professor in the

Continued on page 1118

Continued from page 1104

Dept. of Electrical Engineering, Drexel University. Bilgutay's research activities and interests include ultrasonic testing and imaging, digital signal processing, and communication theory. He is a member of Tau Beta Pi, Eta Kappa Nu, Sigma Xi, ASNT, and IEEE.

J. Saniie received his B.S. in electrical engineering from the University of Maryland, College Park, MD, in 1974, M.S. in biomedical engineering from Case Western Reserve University, Cleveland, OH, in 1977, and Ph.D. in electrical engineering from Purdue University in 1981. In 1981, he joined the Applied Physics Laboratory, University of Helsinki, Finland, to conduct research in photothermal and photoacoustic imaging. Since 1983, Saniie has been with the Dept. of Electrical and Computer Engineering, Illinois Institute of Technology, Chicago, IL, where he is an associate professor and director of the Ultrasonic Information Processing Laboratory. Saniie's current research activities include sonic and radar signal processing, estimation and detection, computer tomography, and ultrasonic imaging with both industrial and biomedical applications. He is a member of IEEE, Tau Beta Pi, Eta Kappa Nu, and Sigma Xi.